



## Experimental Investigations on Microstructural and Mechanical Behavior of Friction Stir Welded Aluminum Matrix Composite

N. Kaushik\*, S. Singhal

Department of Mechanical Engineering, National Institute of Technology, Kurukshetra, Haryana, India

### PAPER INFO

#### Paper history:

Received 05 April 2018

Received in revised form 27 May 2018

Accepted 17 August 2018

#### Keywords:

Aluminum Matrix Composites

Friction Stir Welding

AA6063

Microstructure

Tensile Strength

Hardness

### ABSTRACT

The welding of materials by applying Friction Stir Welding technique is a new solid-state joining technique. The main advantage of this method compared to the traditional joining process is that it minimizes problem-related to metal resolidification as the method incorporates no melting phase. In this experimental work, the effect of friction stir welding (FSW) technique on the microstructure and mechanical properties of the cast composite matrix AA6063 reinforced with 7wt % SiC particles is studied. Friction stir welding, owing to the simultaneous effect of intense plastic deformation and frictional heat generated throughout welding, had impacts each on the reinforcement agents and the matrix alloy. FSW produced a notable reduction in the size of reinforcement agents and their homogeneous distribution in the weld region. It also induced the grain refinement due to dynamic recrystallization of the aluminum matrix alloy in the weld area. The frictional heat generated during friction stir welding had impacts on the growth, dissolution and reprecipitation of the hardening precipitates. The microstructural changes resulted in improved mechanical properties such as UTS, elongation, and hardness of the joint. A joint efficiency of 98.84% was observed for the welded joint. The XRD and EDX analysis of the welded area confirmed that there was no formation of any other compound due to the frictional heat produced during welding. The SEM fracture morphology of the welded joint revealed that the fracture behavior was changed from ductile to brittle following to FSW.

doi: 10.5829/ije.2019.32.01a.21

## 1. INTRODUCTION

Friction stir welding, a solid-state joining process has shown a significant approach for joining of aluminum matrix composites (AMCs). The joining of AMCs by FSW is still a big challenge even though a significant effort has been made in this direction in recent years. Friction stir welding has proven a prominent process in the joining of soft materials (like Al-alloys, AMCs, Mg-alloys), which were difficult to join by the conventional fusion welding processes. Friction stir welding initially was invented and patented by Thomas at TWI (The welding institute) in December 1991 in UK. In this process a non-consumable pin-pointed rotating tool with shoulder moves along the joint line, generating frictional heat and resulting in a flow of plasticized

material near the tool surface. The frictional heat and stirring action of the tool produces a plastic flow in the material, forming a solid-state weld [1-3]. The tool rotational speed and tool transverse speed are the two most important parameters of FSW. The tensile strength of the joint largely depends upon these two parameters. In FSW of AA6063, the tensile strength of the welded joint was increased with increase in tool rotational speed and decreased with increase in tool transverse speed because heat generation due to friction was directly proportional to tool rotation speed [4].

In the early stages, FSW was applied for joining soft metals, Al-alloys such as those of series 2XXX, 6XXX, and 7XXX, which were generally very difficult to weld using conventional fusion welding processes at that time. Aluminum metal matrix reinforced with hard ceramic particles have recently attracted considerable attention in aerospace, shipbuilding, automotive industries and electrical and electronic components etc.

\*Corresponding Author Email: [narinderkaushik83@gmail.com](mailto:narinderkaushik83@gmail.com) (N. Kaushik)

due to their significant mechanical properties over conventional monolithic alloys. The AMCs and PMMCs have a high strength to weight ratio, high specific stiffness, excellent fatigue properties, high corrosion resistant, high formability and improved wear characteristics [5, 6]. It is very difficult to obtain reliable tensile strength and fatigue properties by conventional fusion welding processes due to incomplete mixing of the parent metal and filler material, excessive eutectic formation, porosity and formation of undesirable deleterious phases. The joining of AMC's by applying FSW technique has been explored by a number of researchers as reported in the literature [7, 8]. The various aluminum alloy series like 2XXX, 6XXX and 7XXX strengthened with aluminum oxide ( $Al_2O_3$ ) and silicon carbide (SiC) have been welded in these reported works. The analysis of results confirmed that welded joints of high quality without any visible flaw could be obtained by friction stir welding technique in AMCs strengthened up to 30 wt % reinforcement ceramic agents. Particularly, there was no chemical reaction between the matrix alloy and ceramic phase. Although, it was observed that the material stirring by the rotating tool has a significant impact on the distribution of particles in nugget zone and on the shape and size of reinforcement agents [8]. Microstructural changes and grain refinement have been noticed after FSW. As a result, breakage of reinforcement particles was seen during FSW. The reengagement of particles distribution was seen in the nugget zone for Al-SiC cast composites [8]. Vijay and Murugan [9] analyzed the impact of different tool pin profiles on microscopic examination of friction stir welded AA6061 reinforced with 10 wt %  $TiB_2$  and investigated that the square pin profile produced superior grain structure in the nugget zone which resulted in a higher tensile strength of the joint produced. Chen et al. [10] reported the microstructural examination of friction stir welded AA6063 reinforced with (6, 10.5 vol. %)  $B_4C$  and showed a significant refinement of grains in the nugget zone of the matrix alloy. Guo et al. [11] investigated shattering and smattering of reinforcement particles in FSW of al-alloy AA1100 reinforced with 16 and 30 vol. %  $B_4C$ . Nami et al. [12] studied the influence of tool rotation speed on grain structure of friction stir welded AA6061 reinforced with 15 wt%  $Mg_2Si$  and observed imperfections in the nugget area at high tool rotation rates. Dinaharan and Murugan [13] examined the impact of FSW on the mechanical and microstructural behavior of al-alloy AA6061 reinforced with (0–10 wt %)  $ZrB_2$  and studied that friction stir welding cracked the bunch of reinforcement particles in the as-cast composite into small fine grained particles of various sizes. Langari et al. [14] investigated the impact of tool speed on mechanical properties and weld morphology of FS welded AA7075-T651. It was found that at higher

tool rotation speed and low traverse speed best quality welds were produced. This is due to the minimum tool force at low traverse speed and less shear resistance at higher tool rotational speed. The weld morphology improved by altering the tilt angle from 0 to  $2.5^\circ$ . The hardness value in the SZ increased with increasing traverse speed at a given rotational speed. Zarouni and Eslami [15] studied the TIG welding brazing of AA5083 to steel using Al-5Si as filler and investigated the effect of heat input on the strength of the joints. The microstructural analysis showed that the increase in heat input increased the thickness of IMCs layer appeared at the steel-weld seam interface. Nikoi et al. [16] investigated the impacts of ultrasonic welding process parameters on joint strength of Polypropylene Composite. The impact of three process variables viz., amount of glass fiber in composite, air pressure, welding time and vibration amplitude was analyzed on the tensile strength of the welded joints. The results detailed that maximum failure force of 2.30KN was found when amount of glass fiber is 10%, air pressure is 1.5 bars, welding time is 0.4 s. and vibration amplitude is 32 microns.

A limited amount of work is noticed on the weldability of AA6063/SiC matrix composites by FSW and the evolution of metallurgical and mechanical properties following to FSW. The present research study concentrates on the weldability and microstructural development of AA6063/SiC Al-matrix composites. The attention is focused on the impact of FSW on microstructural features viz., SiC particle distribution, shape and size and grain structure of the welded joint. The macrostructural characteristics clearly recognized the various four zones are also discussed. The mechanical behavior of unreinforced as-cast AA6063, AA6063/7wt % SiC cast composite and AA6063/7wt % SiC welded joint is also evaluated in this study. The XRD and EDX analysis of the welded region have been performed to authenticate the significance of results.

## 2. MATERIAL AND EXPERIMENTAL METHOD

**2. 1. Fabrication of AA6063/SiC Composite** The modified two-step liquid metallurgy processing technique (stir casting process) was employed for the fabrication of proposed AA6063/7wt % SiC aluminum matrix composites. The chemical composition of AA6063 aluminum alloy is shown in Table 1. AA6063 al-alloy was melted at  $810^\circ C$  in a digital temperature controlled top loading electric resistance furnace using a graphite crucible. After entire melting of al-alloy preheated (in a separate furnace at  $900^\circ C$ ) SiC particles in the form of very small packets (enveloped in aluminum foil) were charged into the molten slurry and mechanical stirring at 450 rpm was employed to form a fine vortex [17].

**TABLE 1.** The chemical composition of AA6063 al-alloy

Element	Wt %
Mg	0.96
Si	0.45
Fe	0.35
Cu	0.10
Mn	0.10
Zn	0.10
Cr	0.09
Ni	0.02
Ti	0.01
Al	Remainder

Magnesium metal powder (1% by wt) was mixed into the melt during vortex stirring to improve the wettability between al-alloy and silicon carbide particles. Mechanical stirring of the molten slurry was employed using an SS impeller comprises four blades covered with alumina powder for 15 minutes at an average speed of 450 rpm to ensure the complete mixing of the reinforcement SiC particles into the melt. Two-step stirring procedure was employed to ensure the complete mixing and to overcome problems of agglomeration. The composite slurry at this stage was reheated at temperature  $750\pm 30$  °C, as the temperature lowers down during stirring. At this time mechanical torque was again applied by stirrer and the composite slurry was rotated for 5 minutes at the same average speed. The Composite samples of different wt % (0% and 7%) were obtained by pouring the mixture slurry into preheated (at 250 deg. Celsius) cast iron mold at a pouring temperature of 720 °C and let to cool at room temperature.

## 2. 2. Friction Stir Welding of Composite Plates

The rectangular Plates of size 100mm × 50mm × 6mm (l\*b\*t) were extracted from each casting. The fabrication of butt welding joint of AA6063/7wt% SiC composite plates were carried out on a semi-automatic vertical milling machine (supplied by M/s Bezen Machine Tools, Ludhiana, Punjab, India) by employing a specially designed fixture. The view of the specially designed fixture and the welded composite plate is shown in Figure 1 (a-b). A tool manufactured of AISI H13 tool steel with square pin profile was used for carrying out FSW [9]. The fabricated tool with dimensions is shown in Figure 2 (a-b). The welded joints were produced at a tool rotation rate of 1400 rpm and tool transverse speed of 79 mm/min. The axial load and tool tilt angle have been kept constant at 10KN and 0 degree, respectively. Total Three composite plates were welded to get the average of results. The welding

variables were selected based on a number of test runs to fabricate defect-free welds. In the trial runs some typical friction stir welding defects like pinhole, surface cracks and tunnel defect as depicted in Figure 3, have been observed.

## 2. 3. Mechanical and Microstructural Analysis

Standard specimens were slashed from the welded plates to conduct the mechanical and microscopic examination. To carry out microstructural analysis all the samples were prepared according to a specified metallographic method and etched with Keller's reagent. The scanning electron microscopic examination of the microstructure of prepared welded test samples was done using an SEM analyzer (JSM-6100). The optical microscopic images were captured using an optical microscope (OM) (DEWINTER-Dmi Prime).

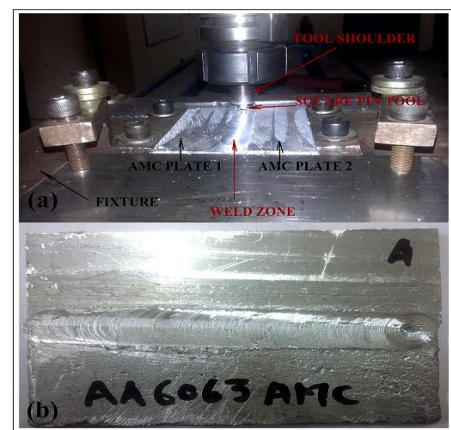


**Figure 1.** (a) View of the fixture and (b) FSW welded plate of AA6063+7 % SiC AMC

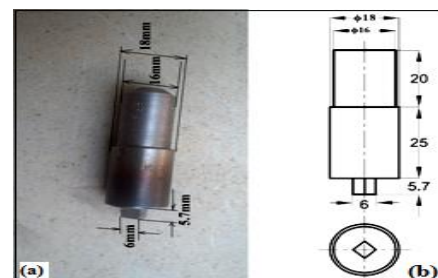


**Figure 2.** (a) FSW tool with square pin profile (b) Tool dimensions

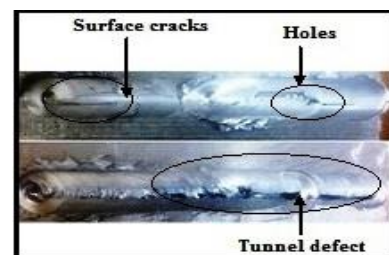


**Figure 3.** Typical defects observed during FSW

XRD analysis was done using Miniflex-II X-ray diffractometer. The EDX analysis of the welded sample was done to know the variation of elements in the weld region using FESEM analyzer. The Vickers microhardness was determined using (FIE model MV1-PC diamond pyramidal indenter) microhardness tester at a fixed load of 0.05kgf applied for a dwell time of 15 seconds. For tensile testing, the samples have been prepared as per ASTM E8M-04 standards as shown in Figure 4. The prepared tensile sample has a gauge length of 40 mm, gauge width of 7 mm and thickness of 6 mm. The UTS of the joint was evaluated utilizing a computerized UTM (FIE UNITEK-94100) of capacity upto 100KN.

### 3. RESULTS AND ANALYSIS

**3.1. Macro And Microstructural Examination of the Welded Joint** AA6063/7wt % SiC composite plates of 6 mm thickness were efficiently butt joined by FSW. The view of the friction stir welded plate is depicted in Figure 1(b). The apex surface of the welded region was specified by semi-circular characteristics similar to those developed in the traditional milling operation. Such characteristics develop due to the rubbing operation of the shoulder of tool and traverse action of the tool on the top surface of the two plates which are to be welded. The apex surface exhibits the plane surface and no cracks, depressions, voids, and immoderate flares are present. It is significant to get a proper apex surface appearance because of the reason that each blemish in the apex heads to some class of flaws in the welded joint.

The macrostructure of AA6063/7wt % SiC composite plate welded joint is shown in Figure 5. The different four zones at macrostructural level are clearly shown in this figure. The macrostructural analysis of the welded joint revealed a continuous flow of material in the plastic state from advancing side (AS) to the retreating side (RS). The FSW defects such as piping, tunnels, and wormhole were not observed. The generation of frictional heat was adequate to transcend the flow stress of the matrix composite to develop a strong welded joint for the specified process variables. The existence of SiC particles limits the free flow of plasticized material in the composite matrix during FSW.

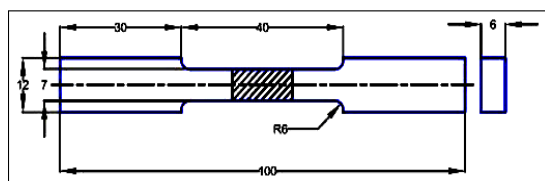


Figure 4. Dimensions of tensile test specimen

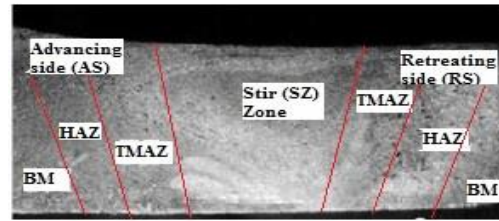
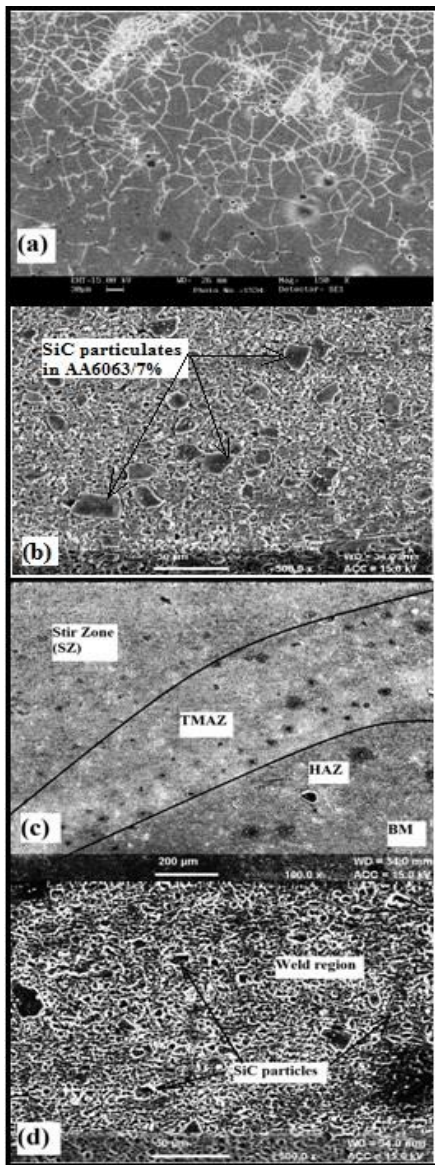


Figure 5. Image showing the different four zones at macrostructure level in welded AA6063/7wt % SiC composite plate

The macrostructure of welded composite plate consists of stir zone (SZ), thermo-mechanically affected zone (TMAZ), heat affected zone (HAZ), and base metal (BM). Thermomechanically affected zone (TMAZ) is the adjoining region of weld region which has undergone plastic deformation due to the influence of thermal cycles. The borderline linking stir zone (SZ) and TMAZ was clearly recognized as small-sized particles appeared in the weld zone due to the influence of stirring action of the rotating tool. The weld zone has been not distinctly recognized by the boundary on the retreating side. Similar examinations were investigated in the literature [18].

The scanning electron microscopic (SEM) images of as-cast AA6063 and AA6063/7wt% SiC matrix composite before and after FSW are shown in Figure 6. The optical images (OM) of AA6063/7wt % SiC composite matrix before and after FSW are also shown in Figures 7 and 8, respectively. In the weld zone, the existence of a large number of small round shaped particles was noticed which were not observed in the base metal composite. The difference in this behavior was due to the stirring action of the tool. The rotating action of the tool wears the surface of SiC particles, promoting the segregation of the sharp edges of the SiC particles, consequently generating small rounded up particles of both larger size particles and debris. This analysis justifies identical investigations on various al-alloy series (6xxx and 7xxx) based metal matrix composites reinforced with various reinforcements [19, 20].

The SEM and OM image of AA6063/7wt % SiC matrix composite as shown in Figures 6(b) and 7, respectively revealed homogeneous dispersion of SiC particles throughout the al-matrix alloy. The majority of SiC particles have been sited in intragranular zones. The clustering of SiC particles was observed in some places. Refinement in grains may be ascribed mainly to the following aspects: (i) SiC particles behave as nucleation locations for grain structure (ii) aluminum matrix grains consolidate on the SiC reinforcement particles [21]. Sufficient mechanical stirring action of the stirrer and consolidation of composite melt throughout casting was attributed to the fine dispersion of SiC reinforcement particles into the composite matrix.



**Figure 6.** SEM images of (a) as-cast AA6063 (b) AA6063/7wt% SiC composite matrix (c) transition zone in the welded joint of AA6063/7wt% SiC (d) Stir zone in the welded joint of AA6063/7wt% SiC

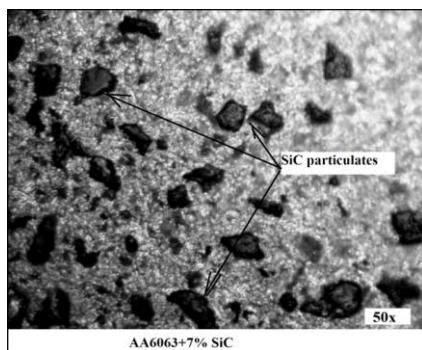


**Figure 7.** Optical images of as-cast AA6063/7wt % SiC matrix composite

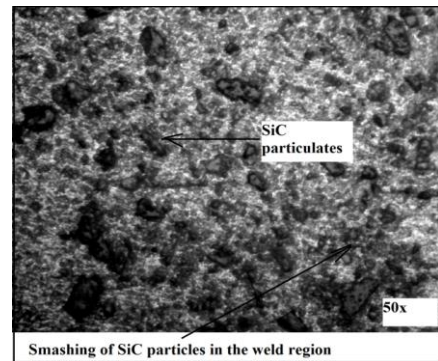


**Figure 8.** Optical image of AA6063/7wt% SiC showing SiC particles in the weld region

The XRD criterion of AA6063/7wt % SiC matrix composite as presented in Figure 9 shows the existence of Al and SiC. No other elements were seen in notable amount. This justifies that no reaction was occurred in between SiC and al-matrix alloy and formation of any other compound was denied. In stir casting the reaction of reinforcement phase and the metal matrix phase sometimes produces unwanted intermetallic compounds which adversely affect the strength of the matrix composite.

The transition zone composed of HAZ and TMAZ is shown in SEM image in Figure 6(c). The SEM analysis showed that the heat affected zone (HAZ) has a close similarity with the parent composite or base metal (BM) zone. A similar grain size and distribution of SiC particles have been observed for HAZ and base metal (BM). Consequently, in friction stir welded aluminum matrix composite, the transition zone can be deemed to be restricted to TMAZ as studied by others [12-13].

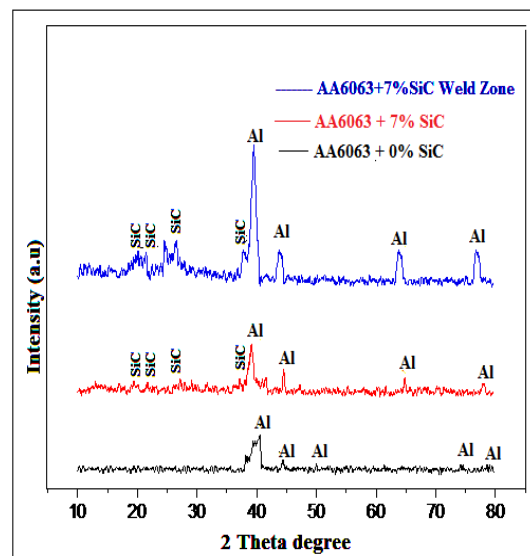


**Figure 9.** XRD analysis of AA6063/7wt% SiC matrix composite and AA6063/7wt% SiC weld region

The exposure of thermal cycles due to frictional heat in the HAZ causes softening behavior. The partition line linking the weld region (stir zone) and TMAZ was distinctly recognizable. TMAZ (Thermo-mechanically affected zone) has experienced severe plastic deformation because of a large amount of frictional heat produced by the rotation of tool under substantial applied axial force. The SEM and OM images of stir zone (weld region) as shown in Figures 6(d) and 8, respectively evidenced that the stir zone has not comprised any porosity or dissociation of SiC reinforcement agents which are susceptible in the conventional fusing welding techniques of al-matrix composites. The stir zone was identified by a homogenous dispersion of SiC particles. During FSW the rotating tool induced intense strain rate in the plasticized material. Consequently, repositioning of the SiC particles occurred during FSW. Bunch of SiC particles of the parent matrix composite fragmented into the homogeneous distribution of SiC particles. The refinement in grains in the stir zone shows dynamic recrystallization throughout friction stir welding (Figures 6-d and 8). The X-ray diffraction (XRD) analysis of the welded area (Figure 9) exhibited no indication of the formation of any other compound except aluminum matrix and SiC particle. There was no reaction occurred between the metal matrix phase and SiC particles due to the frictional heat produced during welding.

The EDX analysis of weld region as shown in Figure 10 confirms the presence of SiC particles and the formation of any other element was denied. The composition of various elements is presented in Table 2. In Table 2, un. C [wt %] = the

Unnormalised concentration in weight percent of the element; norm.C [wt %] = the normalized concentration in weight percent of the element; C Atom. [at. %] the atomic weight percent; (3 Sigma) [wt %] = the error in the weight percent concentration at the 3 sigma level.

**3. 2. Microhardness Examination of the Welded Joint** The graphical analysis of microhardness across the friction stir welded joint in AA6063/7wt % SiC matrix composite is shown in Figure 11.

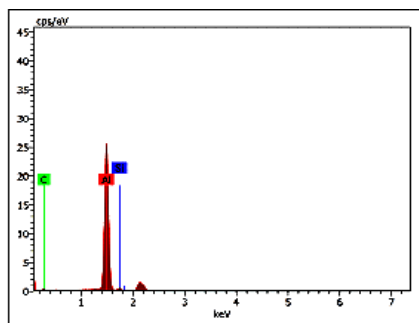


**Figure 10.** EDX analysis of AA6063/7wt% SiC of the welded joint

**TABLE 2.** EDX analysis of AA6063/7wt% SiC of the welded joint

Element Series	unn C [wt%]	norm C [wt%]	Atom C [at%]	Error	3 Sigma [wt%]
Aluminium K-series	39.55	75.16	58.68	5.60	5.60
Carbon K-series	11.90	22.62	39.66	7.93	7.93
Silicon K-series	1.17	2.22	1.67	0.27	0.27
Total	52.62	100.00	100.00	13.80	

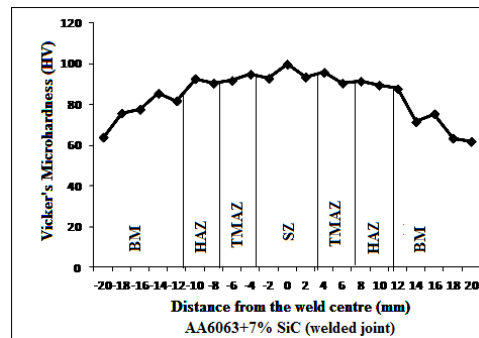


**Figure 11.** Microhardness across the welded joint in AA6063/7wt % SiC matrix composite

A higher value of hardness was observed across the weld area to that of the as-cast composite matrix. This increase in hardness of the welded joint of AA6063/7wt % SiC matrix composite was due to friction stir welding. Hardening of the composite matrix following to FSW has been observed by many researchers [12-13]. The variation in the value of hardness of thermo-mechanically affected zone (TMAZ) and heat affected zone (HAZ) was observed between those of base metal composite and welded region. Compressive stresses have been produced in the plasticized composite matrix by the rotating action of the tool. These compressive stresses minimized the existence of very small sized porosities in the weld region. The fine grain structure observed in the weld region was the outcome of dynamic recrystallization due to high heat generation during FSW in the weld zone. Consequently, The frictional heat generated during friction stir welding resulted in the growth, dissolution, and reprecipitation of the hardening precipitates. The smattering of large SiC particles resulted in increased dislocation density and escort to weld zone hardening. The variation in average vickers microhardness value for the different specimens is shown in Figure 12.

**3. 3. Tensile Behavior of the Welded Joint** The tensile response of as-cast AA6063, AA6063/7wt% SiC composite matrix and AA6063/7wt% SiC welded joint is depicted in Figure 13.

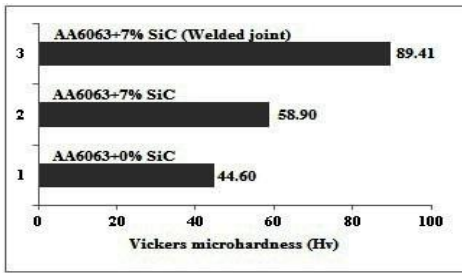


Figure 12. Average Microhardness values for different samples

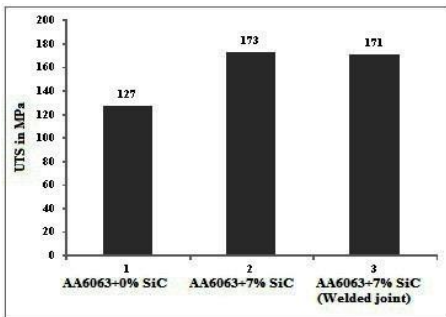


Figure 13. UTS of as-cast AA6063, AA6063/7wt% SiC matrix composite and AA6063/7wt% SiC welded joint

The different specimens after tensile test are shown in Figure 14. The tensile strength of the welded joint was increased significantly by the reinforcement of SiC particles in the al-matrix alloy. The dislocation density has been increased due to the mismatch in coefficient of thermal expansion between the al- matrix and SiC reinforcement particles.

Throughout the tensile loading, the transmission of cracks was opposed by the interaction between the SiC reinforcement particles and dislocation density. The homogeneous dispersal of SiC particles promotes orowan strengthening. The weight carrying capacity of the aluminum matrix composite increased in the absence of voids around SiC particles. Such type of phenomenon results in the strengthening of the matrix composite by the reinforcement of SiC agents into the matrix alloy.

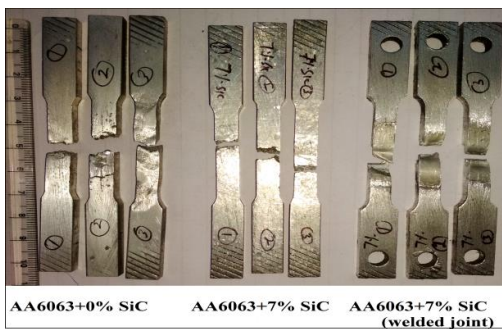


Figure 14. Specimens after tensile test

It was analyzed from Figure 13, that the tensile strength of friction stir welded joint of AA6063/7wt% SiC matrix composite was closer to that of the as-cast AA6063/7wt% SiC matrix composite. In the experimental analysis, a joint efficiency of 98.84% was recorded. The failure of the welded joint has occurred near HAZ. The right selection of welding parameters and defect-free weld region was responsible for this high joint efficiency. The integration of welding parameters yields excellent strengthening of material owing to optimal stirring action, adequate heat production and sufficient introduction of frictional heat and transportation of stirred plasticized material. A decrease in percentage elongation of the joint has been observed as shown in Figure 15, due to the formation of fine grains and smattering of SiC particles in the weld region after FSW.

**3. 4. Fracture Morphology of the Welded Joint**

SEM fracture morphology of as-cast AA6063, AA6063/7wt% SiC matrix composite and welded AA6063/7wt% SiC matrix composite is shown in Figure 16. The fracture morphology of unreinforced (AA6063+0% SiC) as-cast AA6063 al-matrix exhibited a grid of big size depressions as shown in Figure 16(a) and the fracture occurred in a ductile manner. The presence of large size dimples in as-cast AA6063 al-matrix was due to the flow of large amount of material in the plastic state prior to failure. The fracture morphology of as-cast AA6063/7wt % SiC matrix composite as shown in Figure 16(b) exhibited a grid of minor size depressions as compared to the unreinforced as-cast AA6063 matrix alloy. This was due to the decrease in ductility of the matrix composite due to refinement in grains imparted by SiC reinforcement particulates. The fracture morphology of friction stir welded AA6063/7wt% SiC composite joint as shown in Figure 16(c) was recognized by a small number of depressions and the surface was noticed almost regular and flat. The mass flow of plasticized material of composite matrix throughout tensile loading has been negligible and fracture occurred in a brittle manner.

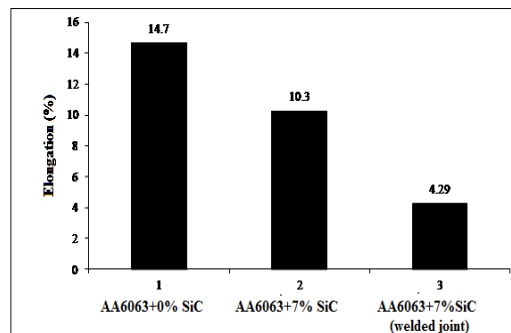
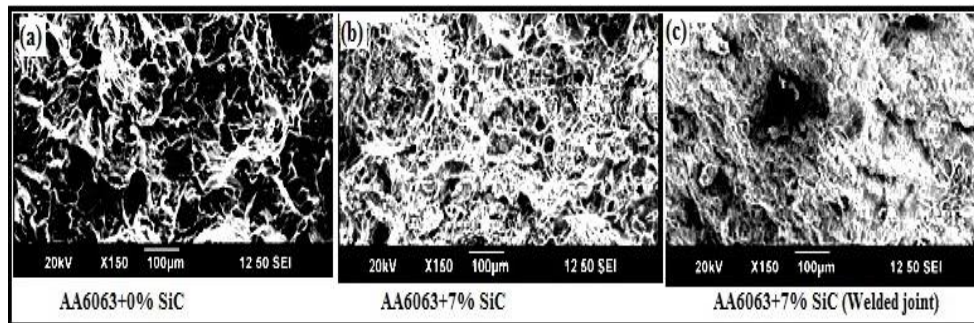


Figure 15. Elongation (%) behavior of as-cast AA6063, AA6063/7wt% SiC matrix composite and AA6063/7wt% SiC welded joint



**Figure 16.** SEM images of fracture surface of: (a) as-cast AA6063 (b) AA6063/7wt % SiC matrix composite (c) Welded AA6063/7wt % SiC matrix composite

#### 4. CONCLUSION

The microstructural analysis of friction stir welded AA6063/7wt% SiC matrix composite joint was characterized into four different zones in accordance with thermal cycles experienced during friction stir welding. (i) Stir zone (SZ) (ii) Thermo mechanically affected zone (TMAZ) (iii) Heat affected zone (HAZ) and (iv) Base metal (BM). HAZ and (iv) base metal region (BM) exhibited very similar characteristics and was very tough to differentiate them. TMAZ exhibited elongated and swiveled grain structure. A homogeneous dispersal of SiC reinforcement particles has been observed throughout the weld area. The bunch of SiC reinforcement particulates of the base metal region or parent composite has been smashed in the weld region by the rotational action of the tool. The microstructural changes in the weld area resulted in high joint efficiency. The experimental states justified that the UTS of the joint has been analogous to the strength of base composite matrix. A reduction in the ductility of the joint was also observed after FSW. The cracking of large size SiC particles after FSW resulted in increased dislocation density and leads to weld zone hardening which resulted in a rise in the hardness value in the weld area as compared to that of the as-cast base metal composite matrix. The increase in hardness in the stir zone is also attributed to the breaking of large SiC particles of the base composite matrix into small fine particles. The fracture behavior has been transformed ductile to brittle succeeding to FSW.

#### 5. REFERENCES

1. Rezaei, G. and Arab, N.B.M., "Investigation on tensile strength of friction stir welded joints in pp/epdm/clay nanocomposites", *International Journal of Engineering-Transactions C: Aspects*, Vol. 28, No. 9, (2015), 1382-1391.
2. Hasanzadeh, R., Azdast, T., Doniavi, A., Babazadeh, S., Lee, R., Daryadel, M. and Shishavan, S., "Welding properties of polymeric nanocomposite parts containing alumina nanoparticles in friction stir welding process", *International Journal of Engineering Transactions A: Basics*, Vol. 30, No. 1, (2017), 143-151.
3. Mishra, R.S. and Ma, Z., "Friction stir welding and processing", *Materials Science and Engineering: R: Reports*, Vol. 50, No. 1-2, (2005), 1-78.
4. Singh, R., Rizvi, S.A. and Tewari, S., "Effect of friction stir welding on the tensile properties of aa6063 under different conditions", *International Journal of Engineering Transactions A: Basics*, Vol. 30, No. 4, (2017), 597-603.
5. Chidambaram, A. and Bhole, S., "Metallographic preparation of aluminum-alumina metal-matrix composites", *Materials Characterization*, Vol. 38, No. 3, (1997), 187-191.
6. Azdast, T. and Hasanzadeh, R., "Tensile and morphological properties of microcellular polymeric nanocomposite foams reinforced with multi-walled carbon nanotubes", *International Journal of Engineering, Transaction C-Aspects*, Vol. 31, (2018), 504-510.
7. Amirizad, M., Kokabi, A., Gharacheh, M.A., Sarrafi, R., Shalchi, B. and Azizieh, M., "Evaluation of microstructure and mechanical properties in friction stir welded a356+ 15% sicp cast composite", *Materials Letters*, Vol. 60, No. 4, (2006), 565-568.
8. Ma, Z., Feng, A., Xiao, B., Fan, J. and Shi, L.K., "Microstructural evolution and performance of friction stir welded aluminum matrix composites reinforced by sic particles", in *Materials science forum*, Trans Tech Publ. Vol. 539, (2007), 3814-3819.
9. Vijay, S. and Murugan, N., "Influence of tool pin profile on the metallurgical and mechanical properties of friction stir welded al-10 wt.% tib2 metal matrix composite", *Materials & Design*, Vol. 31, No. 7, (2010), 3585-3589.
10. Chen, X.-G., Da Silva, M., Gougeon, P. and St-Georges, L., "Microstructure and mechanical properties of friction stir welded aa6063-b4c metal matrix composites", *Materials Science and Engineering: A*, Vol. 518, No. 1-2, (2009), 174-184.
11. Guo, J., Gougeon, P. and Chen, X., "Characterisation of welded joints produced by fsw in aa 1100-b4c metal matrix composites", *Science and Technology of Welding and Joining*, Vol. 17, No. 2, (2012), 85-91.
12. Nami, H., Adgi, H., Sharifitabar, M. and Shamabadi, H., "Microstructure and mechanical properties of friction stir welded al/mg2si metal matrix cast composite", *Materials & Design*, Vol. 32, No. 2, (2011), 976-983.
13. Dinaharan, I. and Murugan, N., "Effect of friction stir welding on microstructure, mechanical and wear properties of aa6061/zrb2 in situ cast composites", *Materials Science and Engineering: A*, Vol. 543, (2012), 257-266.

14. Langari, J., Kolahan, F. and Aliakbari, K., "Effect of tool speed on axial force, mechanical properties and weld morphology of friction stir welded joints of a7075-t651", *International Journal of Engineering*, Vol. 29, (2016), 403-410.
15. Zarooni, M. and Eslami-Farsani, R., "Effect of welding heat input on the intermetallic compound layer and mechanical properties in arc welding-brazing dissimilar joining of aluminum alloy to galvanized steel", *International Journal of Engineering-Transactions B: Applications*, Vol. 29, No. 5, (2016), 669-678.
16. Nikoi, R., Sheikhi, M. and Arab, N.B.M., "Experimental analysis of effects of ultrasonic welding on weld strength of polypropylene composite samples", *International Journal of Engineering-Transactions C: Aspects*, Vol. 28, No. 3, (2014), 447-453.
17. Toptan, F., Kilicarslan, A., Karaaslan, A., Cigdem, M. and Kerti, I., "Processing and microstructural characterisation of aa 1070 and aa 6063 matrix b4cp reinforced composites", *Materials & Design*, Vol. 31, (2010), S87-S91.
18. Minak, G., Ceschini, L., Boromei, I. and Ponte, M., "Fatigue properties of friction stir welded particulate reinforced aluminium matrix composites", *International Journal of Fatigue*, Vol. 32, No. 1, (2010), 218-226.
19. Baxter, S. and Reynolds, A., "Characterization of reinforcing particle size distribution in a friction stir welded al-sic extrusion", *Lightweight Alloys for Aerospace Application*, (2001), 283-293.
20. Prado, R., Murr, L., Shindo, D. and Soto, K., "Tool wear in the friction-stir welding of aluminum alloy 6061+ 20 al 2 o 3: A preliminary study", *Scripta Materialia*, Vol. 1, No. 45, (2001), 75-80.
21. Kumar, B.A. and Murugan, N., "Metallurgical and mechanical characterization of stir cast aa6061-t6-alnp composite", *Materials & Design*, Vol. 40, (2012), 52-58.

## Experimental Investigations on Microstructural and Mechanical Behavior of Friction Stir Welded Aluminum Matrix Composite

N. Kaushik, S. Singhal

Department of Mechanical Engineering, National Institute of Technology, Kurukshetra, Haryana, India

### PAPER INFO

چکیده

#### Paper history:

Received 05 April 2018

Received in revised form 27 May 2018

Accepted 17 August 2018

#### Keywords:

Aluminum Matrix Composites

Friction Stir Welding

AA6063

Microstructure

Tensile Strength

Hardness

جوشکاری مواد با استفاده از تکنیک جوش اصطکاکی یک روش اتصال جدید حالت جامد است. مزیت اصلی این روش نسبت به روند پیوستن سنتی این است که آن را به مسائل مربوط به بازسازی فلزات می رساند، زیرا این روش شامل هیچ مرحله ذوب نمی شود. در این کار آزمایشی اثر تکنیک جوشکاری اصطکاکی (FSW) بر روی ریزساختار و خواص مکانیکی ماتریس کامپوزیتی AA6063 تقویت شده با 7wt % SiC ذرات مورد مطالعه قرار گرفته است. جوشکاری اصطکاکی با توجه به اثر همزمان تغییر شکل شدید پلاستیکی و گرمای اصطکاک تولید شده در طی جوشکاری، هر کدام بر روی آلیاژهای تقویت کننده و آلیاژ ماتریکس تأثیر می گذارد. FSW کاهش قابل توجهی در اندازه عوامل تقویت کننده و توزیع همگن آنها در منطقه جوش ایجاد کرد. همچنین با توجه به پراکندگی پویا آلومینیوم ماتریس آلومینیومی در منطقه جوش، پالایش دانه را القا می کند. گرمای اصطکاکی که در طی جوشکاری اصطکاک جوشکاری ایجاد شده، بر رشد، انحلال و جایگزینی رسوبات سخت افزاری تأثیر گذاشته است. تغییرات ریز ساختاری منجر به بهبود خواص مکانیکی مانند UTS، انقباض و سختی مفصل می شود. بازده مشترک 98.84٪ برای جوش داده شده بود. تجزیه و تحلیل EDX و XRD در منطقه جوش نشان داده شده است که هیچ ترکیب دیگری به علت گرمای اصطکاک تولید شده در جوشکاری ایجاد نشده است. مورفولوژی شکستگی SEM جوش داده شده نشان داد که رفتار شکستگی از مجذور به شکننده پس از FSW تغییر کرد.

doi: 10.5829/ije.2019.32.01a.21